



KOH-promoted Pt/Al₂O₃ catalysts for water gas shift and methanol steam reforming: An operando DRIFTS-MS study



Andre Kaftan^a, Matthias Kusche^b, Mathias Laurin^a, Peter Wasserscheid^{b,c}, Jörg Libuda^{a,c,*}

^a Lehrstuhl für Physikalische Chemie II, Friedrich-Alexander-Universität Erlangen-Nürnberg, Egerlandstr. 3, 91058 Erlangen, Germany

^b Lehrstuhl für Chemische Reaktionstechnik, Friedrich-Alexander-Universität Erlangen-Nürnberg, Egerlandstr. 3, 91058 Erlangen, Germany

^c Erlangen Catalysis Resource Center, Friedrich-Alexander-Universität Erlangen-Nürnberg, Egerlandstr. 3, 91058 Erlangen, Germany

ARTICLE INFO

Article history:

Received 20 May 2016

Received in revised form 2 August 2016

Accepted 4 August 2016

Available online 6 August 2016

Keywords:

Infrared spectroscopy

Online mass spectrometry

Platinum

Water-gas shift

Methanol steam reforming

ABSTRACT

The performance of KOH-modified Pt/Al₂O₃ catalysts has been investigated under the conditions of the water-gas shift (WGS) reaction and methanol steam reforming (MSR) with diffuse reflectance infrared Fourier-transform spectroscopy (DRIFTS) coupled with online quadrupole mass spectrometry (QMS). We demonstrate that both the activity and the selectivity are enhanced in comparison to the uncoated catalyst by applying a thin coating of KOH. By means of IR spectroscopy, we were able to follow the formation of surface species on two different types of catalysts. During reaction, primarily formates are observed on the uncoated catalyst while a film of hydroxides and carbonates is observed on the KOH-coated sample. Additionally, the vibrational bands of CO adsorbed on Pt suggest a strong modification of the electronic structure of the Pt particles by K-coadsorption, leading to a weakening C—O bond and a strengthening of the Pt—C bond. As a result, we observe an increased selectivity to CO₂ on the KOH modified system.

© 2016 Elsevier B.V. All rights reserved.

1. Introduction

In the future transition towards renewable energy sources, hydrogen is generally considered to be among the most important energy carriers [1,2]. Among the chemical hydrogen storage materials, methanol is a high potential candidate with a hydrogen storage capacity of 12.5 wt%. In contrast to compressed hydrogen, methanol is a relatively safe and easy-to-handle fuel [3]. Molecular hydrogen can be released from methanol by methanol steam reforming (MSR), converting methanol and water into carbon dioxide and hydrogen.

In practice steam reforming does not exclusively yield H₂ and CO₂, but also produces CO via methanol decomposition. CO formation does not only reduce the H₂ yield, but also makes additional purification steps necessary, for example, for the use of H₂ in PEM

(proton exchange membrane) fuel cells, where only traces of CO are acceptable [4]. Typically the CO and the CO₂ concentration in the gas phase are coupled via the water-gas shift (WGS) reaction and catalysts which are active in MSR are often also active for the WGS reaction. The most common catalyst, alumina-supported Cu/ZnO, shows high activity and selectivity, but also has major drawbacks such as the need for lengthy activation procedures and special treatment to avoid deactivation during standby as well as its pyrophoric nature [5]. Alternative catalysts for steam reforming are based on oxide-supported noble metal particles, specifically Pt or Pd. These catalysts are easier to handle and show instant start-up behavior, but their catalytic performance lags far behind the commercial Cu-based systems so that in most applications their advantages do not justify the higher costs [6,7].

Recently, several studies demonstrated increased activity and selectivity of alkali-modified noble metal catalysts for the use in WGS and MSR. Liu et al. found that the addition of K₂CO₃ balances the concentration of water and CO on the Ru/C-catalysts and, thereby, significantly improves the activity and the selectivity of the WGS reaction [8]. Zhai et al. found that surface OH can be stabilized by alkali ions on alumina-supported Pt, and they associated this property to the low-temperature WGS activity [9]. Other studies suggested that the C—H bond strength of formate and methoxy

* Corresponding author at: Lehrstuhl für Physikalische Chemie II, Friedrich-Alexander-Universität Erlangen-Nürnberg, Egerlandstr. 3, 91058 Erlangen, Germany.

E-mail addresses: andre.kaftan@fau.de (A. Kaftan), matthias.kusche@crt.cbi.uni-erlangen.de (M. Kusche), mathias.laurin@fau.de (M. Laurin), peter.wasserscheid@fau.de (P. Wasserscheid), joerg.libuda@fau.de (J. Libuda).

intermediates is decreased during WGS and MSR by the addition of alkali ions. This effect was reported to yield higher activities on zirconia or ceria supported Pt catalysts [10,11]. Several extensive surface science studies also confirmed the major influence of alkali doping on the metal–CO interaction. These studies indicated a drastic weakening of the CO bond and increased bonding strength for the Pt–C bond [12–14]. However, there is still some debate on the role of the alkali dopant. For instance, Pazmino et al. observed an increased WGS activity for Na-modified Pt on Al_2O_3 and TiO_2 and suggested that the promoting effect is due to a modification of the support by the alkali atom which creates active sites on the support itself [15].

In this work we investigate a commercial Pt/alumina catalyst which is additionally modified by applying a thin KOH-coating in a wet-chemical approach. This coating is performed in a simple, synthetically straightforward, and economically attractive way. In earlier publications we already demonstrated that the modification procedure yields a significantly enhanced activity and selectivity for the catalysts applied in WGS and MSR [16–18]. Catalysts modified in this way show improved turn-over-frequencies (TOF) by a factor of up to 5. Most importantly, however, the catalysts show outstanding selectivities for CO_2 which are improved from about 50% on the neat catalyst to more than 99% under identical conditions in the presence of the KOH. We found that the most active and most selective catalyst was Pt/ Al_2O_3 coated with 7.5 wt% KOH. In this work we aim at a spectroscopic characterization of the KOH-modified Pt/ Al_2O_3 catalyst under the conditions of MSR. Specifically, we use operando diffuse reflection infrared Fourier-transform spectroscopy (DRIFTS) combined with online quadrupole mass spectrometry (QMS) to monitor how changes at the surface of the noble metal or the support are related to changes on the composition of the product gas stream. Noteworthy, this technique allows us to investigate the catalyst without any further modification under conditions that are relatively close to the “real” reaction conditions.

2. Experimental

2.1. Catalyst preparation

Pt on aluminum oxide ($\gamma\text{-Al}_2\text{O}_3$) was purchased from Alpha Aesar (LOT: F02R004, Pt content = 4.86 wt%). KOH (>85%, rest H_2O , K_2CO_3 <1%) was purchased from Merck. For the preparation, Pt/ Al_2O_3 was immersed into a solution of the KOH in high-purity water (typically 20 mL). After stirring for 30 min at 25 °C, the solvent was removed under vacuum (4 h, 150 °C, <0.1 mbar). The exact amount of hydroxide was determined by subsequent titration with 1 M HCl (Merck). In this work, the salt loading was 17.2 wt% based on the whole mass of the catalyst. The reason for this relatively high loading is to reduce the amount of uncoated sites on the catalyst while mass transfer barriers are not greatly influencing the reaction. Further information about the catalyst preparation and characterization can be found in earlier publications [16–18]. For completeness, we would like to summarize briefly the main properties of these catalysts. The untreated Pt/ Al_2O_3 catalysts have a mean particle diameter of 2.7 nm (corresponding to a Pt dispersion of 37%) while on the KOH-treated samples a mean diameter of 5 nm was found (determined by high resolution transmission electron microscopy) [18]. The agglomeration is partly reversible under the conditions of the WGS reaction and the coated catalysts show a mean Pt particle diameter of 3.0 nm after 240 h under WGS conditions. Furthermore, it was shown that K^+ is homogeneously distributed on the Al_2O_3 surface and is in close contact to Pt particles.

2.2. Operando DRIFTS–mass spectrometry measurements

The operando experiments have been performed in a Bruker Vertex 80v IR spectrometer equipped with a specially modified sample compartment. The operando setup provides all necessary gas in- and outlets and allows for temperature measurement and control. Very importantly the optical path is kept evacuated during the complete measurement. For DRIFTS, we used a high-temperature reaction chamber (Harrick, HVC-DRP-5) fitted with CaF_2 windows and a Praying Mantis diffuse reflection accessory (Harrick). Temperatures were directly measured in the center of the catalytic bed by means of a 0.34 mm diameter type K thermocouple [19]. Mass flows and pressures were regulated using mass flow and pressure controllers (Bronkhorst).

The vapor of water (Millipore water, >18 MΩ) and methanol (Sigma-Aldrich, BioReagent, ≥99.93%) were dosed onto the samples using a liquid bubbler system with Ar as a carrier gas. Both liquids have been purified prior to usage by several freeze-drying cycles. The vapor pressure was controlled with a temperature bath and was set to 20 °C (23 mbar) for H_2O and 0 °C (40 mbar) for MeOH [20]. Prior to the experiments, the catalyst powder was heated under an Ar flow (5 $\text{mL}_\text{N}\text{ min}^{-1}$, 100 mbar) at 350 °C for 30 min to desorb water and other contaminants. IR spectra were recorded with a spectral resolution of 2 cm^{-1} , 151 scans, and a scanning speed of 40 kHz which yields an acquisition time of 60 s per spectrum or equivalently 1 spectrum per 10 °C. The IR data are shown in absorbance units (-log R), where R is the sample reflectance, since the Kubelka-Munk function does not provide a good linear correlation of band intensity vs surface coverage for strongly absorbing samples as Pt/ Al_2O_3 [21,22].

The total pressure of the reactor system was maintained at 100 mbar. This relatively low pressure is necessary to reduce the response time between the exit of the gases from the reactor and their detection by the mass spectrometer. After the reactor, a small amount of the exhaust gas stream was split using a fine leak valve to the inlet of a quadrupole mass spectrometer (Hiden Analytical HAL 301) operated at a pressure of 3×10^{-7} mbar (base pressure < 2×10^{-10} mbar). The measured signals were normalized to the Ar signal in order to compensate for the effects due to variations in the total pressure at the mass spectrometer level for experiments on the different samples as well as for drifts in the mass spectrometer sensitivity between the experiments. The background pressure was subtracted from all measured masses. Relative sensitivity factors and fragmentation patterns have been determined by measuring gas mixtures with known composition. The QMS data shown here were corrected by these factors and contributions from fragmentation were subtracted. The following m/z values were used: H₂, 2; CH₄, 15; H₂O, 18; MeOH, 31; Ar, 40; CO₂, 44. For better visibility, the data for H₂ is scaled by a factor of 0.33.

All gases were used without further purification (Ar, Linde, >99.999%; CO, Linde, >99.997%).

2.3. TP-IR CO-DRIFTS

After taking a reference spectrum at 50 °C in Ar atmosphere, a diluted stream of CO (20% in Ar) was dosed onto the samples for 10 min until the intensities of new features were constant. Subsequently the reactor was purged for at least 30 min with an Ar flow (5 mL min^{-1}) to remove residual CO from the gas-phase. IR spectra (acquisition time: 1 min) were recorded in a time- and temperature-programmed fashion during a linear heating ramp (10 K min⁻¹) to 350 °C.

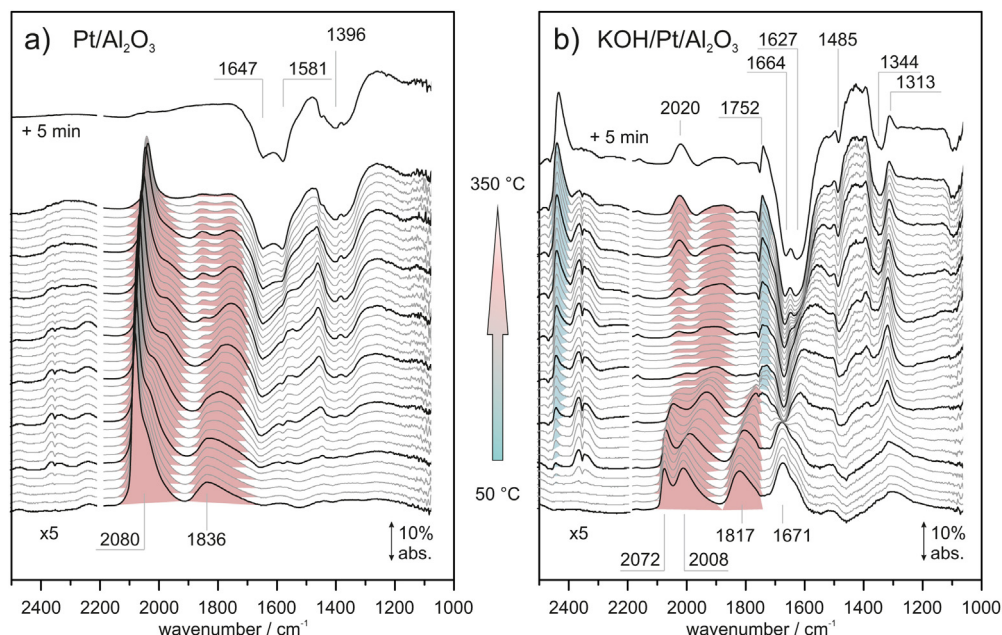


Fig. 1. DRIFT spectra of CO adsorbed on (a) Pt/Al₂O₃ and (b) KOH/Pt/Al₂O₃. The temperature was ramped linearly during the experiment (10 K min⁻¹) from 50 to 350 °C. Bold lines indicate spectra separated by 50 K. The reference spectrum was recorded prior to CO dosage at 50 °C.

2.4. Water gas shift reaction

A reference spectrum was taken at 50 °C in Ar atmosphere. Subsequently, a mixture of 10% H₂O and 11% CO in Ar (total flow: 4 mL_N min⁻¹) was passed through the catalyst bed until the IR spectra and the QMS signals stabilized. IR spectra (acquisition time: 1 min) were recorded in a time- and temperature-programmed fashion during a linear heating ramp (10 K min⁻¹) to 350 °C. For the QMS data, the subsequently recorded cooling ramp (10 K min⁻¹) is also shown in semi-transparent colors. Catalyst activities are given as turnover frequencies (TOF), which is the total molar flow of CO₂ divided by the total molar amount of Pt in the reactor (about 1×10^{-5} mol). A Pt dispersion of 37% was considered [16].

2.5. Methanol steam reforming

A reference spectrum was taken at 50 °C in Ar atmosphere. Subsequently, a mixture of 3.3% MeOH and 6.7% H₂O in Ar (total flow: 3 mL_N min⁻¹) was passed through the catalyst bed until the IR spectra and the QMS signals stabilized. IR spectra (acquisition time 1 min) were recorded in a time- and temperature-programmed fashion during a linear heating ramp (10 K min⁻¹) to 350 °C. For the QMS data, the subsequently recorded cooling ramp (10 K min⁻¹) is also shown in semi-transparent colors. Catalyst activities are given as TOF, which is the total molar flow of CO, CO₂, and CH₄ divided by the total molar amount of Pt in the reactor (typically 1×10^{-5} mol). Selectivities for CO₂ are given as the mole fraction of CO₂ in the outlet gas stream divided by the sum of the moles of CO₂, CO, and CH₄. A Pt dispersion of 37% was considered.

3. Results and discussion

3.1. Temperature-programmed DRIFTS: CO/KOH-Pt/Al₂O₃

First, we discuss the results of our temperature-programmed DRIFTS (TP-DRIFTS) experiments for CO on pristine and KOH-coated Pt/Al₂O₃ catalysts. CO is a well-known probe molecule for metallic substrates and gives insight into modifications of binding sites or the electronic structure.

Fig. 1a) shows the TP-DRIFTS spectra for Pt/Al₂O₃. After CO dosage at 50 °C (bottom spectrum), two peaks at 2080 and 1836 cm⁻¹ (highlighted in red) and a minor shoulder at 2060 cm⁻¹ can be detected. During heating, the intensity of the 2080 cm⁻¹ signal and its shoulder (2060 cm⁻¹) decreases gradually and the peak positions shift slightly to lower wavenumbers (2036 cm⁻¹ and 2000 cm⁻¹, resp.). The behavior of the broad signal at 1836 cm⁻¹ is quite similar. This peak shifts from 1836 cm⁻¹ at 50 °C to a frequency of 1760 cm⁻¹ at 200 °C. Additionally, during heating, three negative features centered at 1647, 1581, and 1396 cm⁻¹ can be observed. While holding the catalyst at 350 °C for additional 5 min after the end of the ramp the signal at 2036 cm⁻¹ vanishes completely.

We can assign the signal at 2080 cm⁻¹ to CO molecules adsorbed linearly on terraces and its shoulder at the low frequency side to CO adsorbed linearly on lower coordinated Pt atoms (edges or corners) of the nanoparticles [23–25]. The broad band at 1836 cm⁻¹ represents CO adsorbed in bridge conformation on Pt terraces. Note that the abundance of the species are not directly reflected by the intensities due to dipole coupling and intensity transfer [26,27]. The signal at 1647 cm⁻¹ can be attributed to residual water desorbing from the support [28]. The other two broad signals at 1582 and 1396 cm⁻¹ originate from the decomposition of different mono- and bidentate carbonates or carboxylates which were formed during the preparation of the catalyst [29,30]. These species decompose during heating and form CO₂ which can be seen as a weak gas-phase signal around 2340 cm⁻¹. By holding the catalyst at 350 °C for additional 5 min after the end of the ramp it is even possible to desorb the remaining CO from Pt.

For the KOH treated sample (Fig. 1b), four distinct peaks at 2072, 2008, 1817 and 1671 cm⁻¹ can be observed after CO dosage at 50 °C. During heating, several positive bands (2435, 2020, 1742, and 1313 cm⁻¹) and negative bands (1752, 1627, 1485, and 1344 cm⁻¹) appear. The three bands at higher frequencies after CO exposure (2072, 2008, and 1817 cm⁻¹; highlighted in red) show a similar shift to lower wavenumbers during the heating ramp.

Most importantly the peaks in the CO stretching region look very different on the KOH-treated catalyst. Two bands in the stretching frequency region of linear CO are found at 2072 and 2008 cm⁻¹.

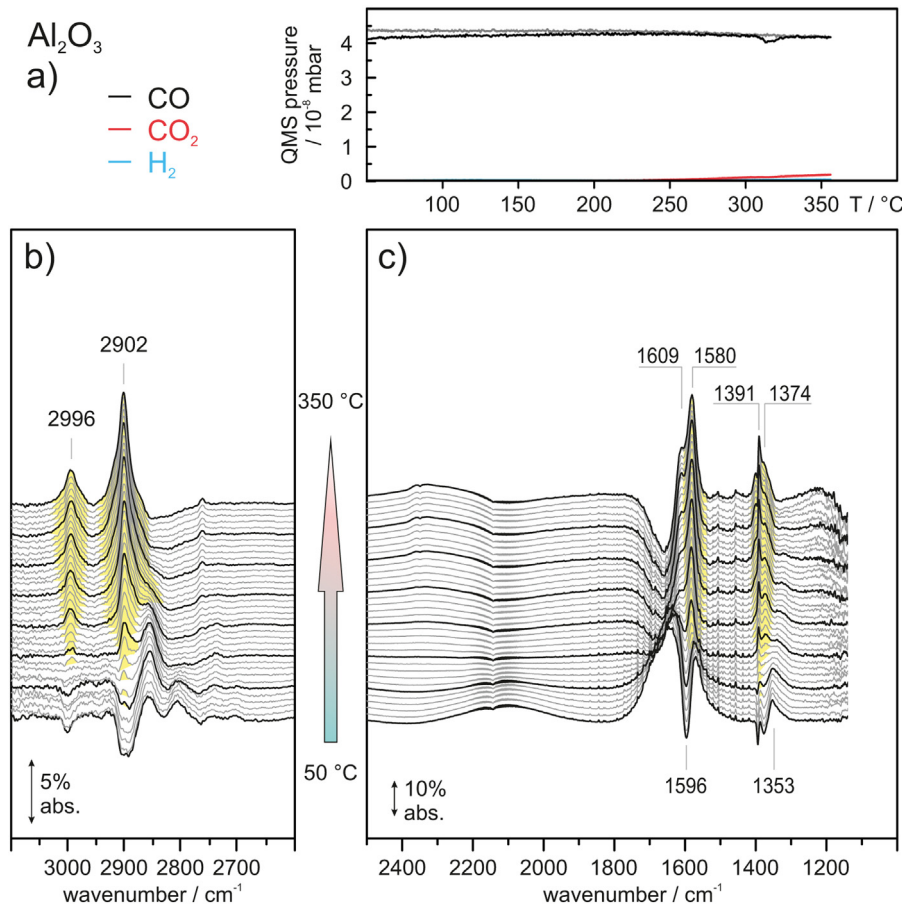


Fig. 2. Online QMS (a) of Al_2O_3 during temperature-programmed (10 K min^{-1}) WGS reaction and corresponding DRIFT spectra (b and c). Bold lines indicate spectra separated by 50°C . The reference spectrum was recorded prior to H_2O and CO dosage at 50°C .

These peaks can be assigned to CO adsorbed linearly (atop) on Pt-atoms (2072 cm^{-1}) and K-influenced Pt-atoms (2008 cm^{-1}), respectively. The origin of the splitting of the atop-signal has been discussed previously [16,17,31]. The new CO signal is associated with linear CO on Pt-atoms which are influenced by K-atoms. The co-adsorbed K increases the electron density in the Pt d-bands and thereby enhancing electron transfer from the d-bands to the antibonding 2π orbitals of CO [31]. As a result the C–O bond is weakened and shifts to lower frequencies while the Pt–C bond is strengthened [12–14]. The lower intensity of the linear band at 2072 cm^{-1} and the higher intensity of the bridge band at 1817 cm^{-1} compared to pristine Pt/ Al_2O_3 (Fig. 1a) suggest an alkali-induced displacement of CO from atop at terraces and particle edges to bridging sites at terraces (1817 cm^{-1}).

The new band at 1671 cm^{-1} decreases steadily during the heating ramp and becomes negative, indicating a species already present before CO adsorption. We assign this band to water which adsorbed on the catalyst after the pretreatment, since the KOH-coating is highly hygroscopic.

During heating of the sample, the signals assigned to CO adsorbed on Pt severely shift to lower frequencies and lose the majority of their initial intensity. This behavior suggests a rapid removal of CO from Pt. We explain this by the presence of large quantities of OH groups on the highly hygroscopic and alkaline sample. Excess OH⁻ then reacts with CO on Pt to CO_2 , whose evolution can be seen at 2340 cm^{-1} . This process starts at relatively mild temperatures around 150°C , suggesting considerably improved activity for the WGS reaction. With the temperature increasing further, the formation of carbonates at 1313 cm^{-1} can

be observed, and the broad negative feature around 1650 cm^{-1} suggests the removal of large quantities of water, either via desorption or by consumption by the WGS reaction. The lack of gas phase H_2O bands in the range of 1800 – 1400 cm^{-1} endorses that H_2O rather reacts with CO, however. Surprisingly, a new feature in the Pt–CO region at 2020 cm^{-1} arises. We propose that, at this stage of the experiment, water and hydroxyl groups are depleted on the catalyst. The formed carbonates subsequently decompose at elevated temperatures to CO_2 which can dissociate on K-modified Pt to form adsorbed CO and O [32]. CO on Pt at low coverages adsorbs preferentially on defect sites and thereby causes the band at 2020 cm^{-1} [33]. At the highest temperature of 350°C , the presence of two additional features at 2435 and 1752 cm^{-1} (blue) can be seen. These signals develop over the whole course of the experiment and can be assigned to combination bands of the carbonate anion of K_2CO_3 [34–36]. After further 5 min at 350°C , the signals of CO on Pt (2020 cm^{-1}) as well as the K_2CO_3 combination bands (2435 and 1752 cm^{-1}) show no decrease in intensity demonstrating the high stability of these species. This observation is in good agreement with earlier surface science studies of CO adsorbed on K-modified Pt, where temperature-programmed desorption (TPD) shows an enhanced stability of CO adsorbed on Pt [31,37].

3.2. Water gas shift reaction

To study the influence of the K-salt on the catalytic performance for WGS, we performed online-quadrupole mass spectrometry (QMS) combined with in situ DRIFTS. Samples with and without Pt and KOH-coated and uncoated were investigated in a

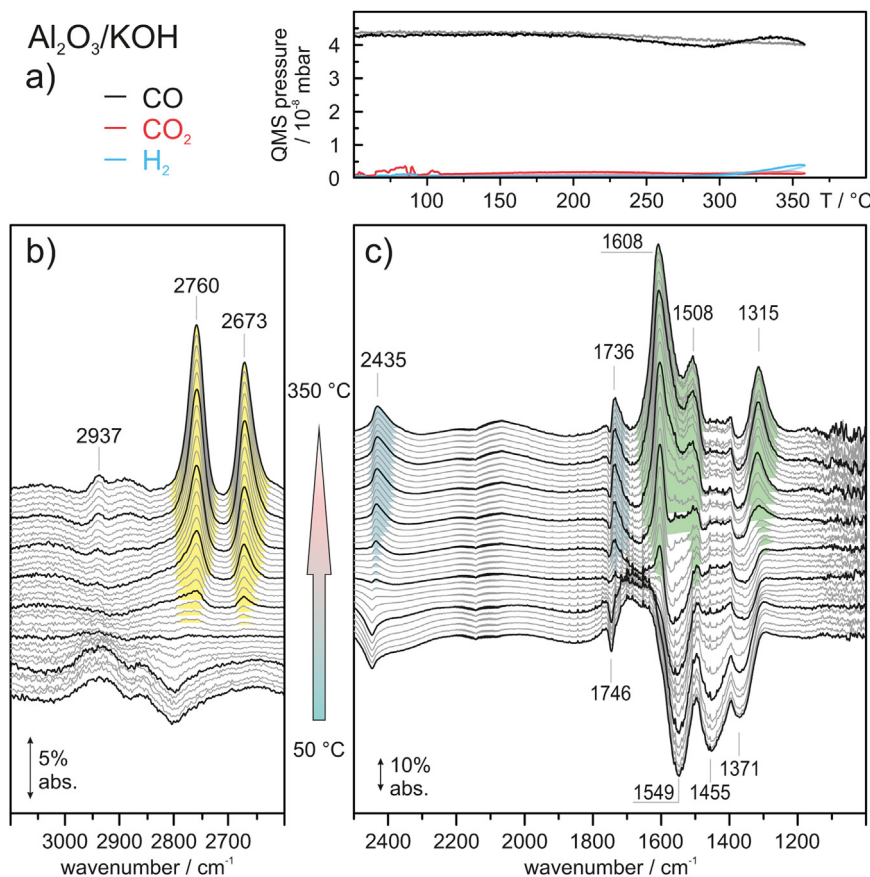


Fig. 3. Online QMS (a) of KOH-treated Al₂O₃ during temperature-programmed (10 K min⁻¹) WGS reaction and corresponding DRIFT spectra (b and c). Bold lines indicate spectra separated by 50 °C. The reference spectrum was recorded prior to H₂O and CO dosage at 50 °C.

temperature-programmed experiment with a constant feed of 11% CO and 10% H₂O in Ar.

3.2.1. Al₂O₃

Fig. 2a) shows the QMS data of the reference sample Al₂O₃ without KOH-coating. As expected, no significant CO conversion could be observed for the Pt and K-salt free sample. A small amount of CO₂ can be detected at elevated temperatures, most likely from residuals of the preparation. DRIFT spectra of this sample in Fig. 2b) show the formation of two bands in the C–H stretching region which can be assigned to the C–H stretching mode (2902 cm⁻¹) and a combination band (2996 cm⁻¹) of formate species formed on the surface [38]. The signals in the region between 2500 and 1000 cm⁻¹ (Fig. 2c) confirm this observation. During heating of the catalyst water desorbs (very broad signal centered around 1640 cm⁻¹) and the exposed surface of Al₂O₃ can react with CO from the feed to form surface bound formates. This can be seen by the evolution of new bands at 1580, 1391, and 1374 cm⁻¹ which can be assigned to $\nu_{as}(OCO)$, $\nu_s(OCO)$, and $\delta_{inplane}(OCH)$ of formate bound to the alumina surface [38,39]. This behavior is in excellent agreement with previously reported studies of MeOH adsorption on Al₂O₃ [40].

3.2.2. KOH/Al₂O₃

The corresponding spectra and QMS measurements of the Al₂O₃ sample coated with KOH are shown in Fig. 3. Similar to the uncoated sample, no significant CO₂ or H₂ production can be observed in the QMS data (Fig. 3a). Only a small drop of CO concentration in the product stream at temperatures above 200 °C without simultaneous evolution of CO₂ may indicate a conversion of CO to surface bound species. IR spectra in the range of 3100–2600 cm⁻¹ confirm this assumption. Two intense bands at 2760 and 2673 cm⁻¹

(yellow) develop at temperatures above 200 °C. These bands occur at frequencies which are rather untypical for C–H stretching vibrations. Early assignments attribute these bands to the formation of potassium formates. [41–43] Similar band positions for formates during WGS reactions have been reported for K-doped Pt/ZrO₂ catalysts. The authors explain this by a significant weakening of the C–H bond strength of surface-bound formates induced by the alkali metal [10,44]. After the dosage of water and CO onto the sample, negative bands in the fingerprint region at 2435, 1746, 1548, 1455, and 1371 cm⁻¹ are observed (Fig. 3c). We assigned the bands at 2435 and 1746 cm⁻¹ (blue) already to overtone vibrations of K₂CO₃. As shown in the TP-DRIFTS spectra for KOH/Pt/Al₂O₃, K₂CO₃ is very stable and formed in large amounts at high temperatures. Thus we assume that, upon addition of H₂O, K₂CO₃ decomposes to form CO₂ and OH. The other bands (green) can be attributed to symmetric and asymmetric stretching vibrations of the carbonate ion in the K-salt and to surface bound carbonates. During heating under WGS conditions, the negative features gain in intensity again, showing the formation of the previously decomposed carbonates while consuming a part of CO from the gas feed.

3.2.3. Pt/Al₂O₃

Fig. 4a) shows the QMS spectra of the WGS reaction on Pt/Al₂O₃. The conversion of CO to CO₂ is observed at temperatures above 200 °C accompanied by evolution of H₂. Equilibrium conversion is achieved at 350 °C and the TOF increases to 227 h⁻¹.

In the IR spectra, only two minor peaks (yellow) develop in the C–H region (Fig. 4b) at temperatures around 200 °C. The signals appear at the same positions as previously seen for formate on the pristine Al₂O₃ samples, but with greatly reduced intensities. In

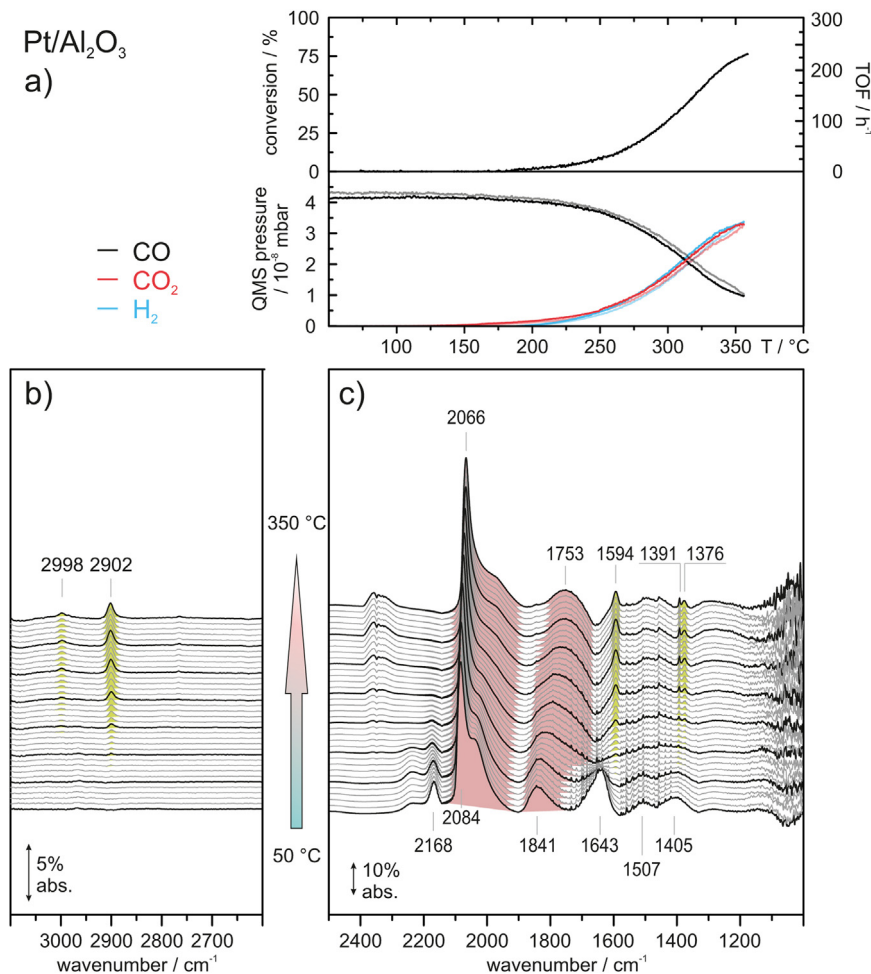


Fig. 4. Online QMS (a) of Pt/Al₂O₃ during temperature-programmed (10 K min⁻¹) WGS reaction and corresponding DRIFT spectra (b and c). Bold lines indicate spectra separated by 50 °C. The reference spectrum was recorded prior to H₂O and CO dosage at 50 °C.

the range between 2500 and 1000 cm⁻¹ (Fig. 4c), several signals at 2168, 2064, 1841, 1643, 1507, and 1405 cm⁻¹ develop after dosing H₂O and CO onto the sample. The signal at 2084 cm⁻¹ is attributed to CO adsorbed atop on Pt. The frequency here is slightly higher than it was observed after dosing CO without water on Pt (2072 cm⁻¹). Additionally, a shoulder at lower frequency shows CO molecules occupying low-coordinated Pt atoms (kinks, edges and step-sites) of the particles. The signal of CO bound to Pt in bridge-bonded configuration can be found at 1841 cm⁻¹. The vibrations of adsorbed water can be seen at 1643 cm⁻¹ and another sharp and small feature is observed at 2168 cm⁻¹. Typical frequencies reported for CO adsorbed linearly on Pt are in the range of 2100–2050 cm⁻¹ [23–25]. For the adsorption of CO on oxidized Pt particles an increase of the CO vibration frequency can be observed, but these shifts are rather small compared to our observation and typical frequencies are around 2130 cm⁻¹ [45]. Another possible explanation could be the co-adsorption of CO with adsorbates. Here, we dosed water onto the surface first and then CO. It is known that water dissociates on Pt to form surface bound OH and H species [46]. These co-adsorbates have different effects on the frequency of the CO vibration. While the presence of electron withdrawing adsorbates (such as OH or O) shifts the vibrational frequency of CO to higher wavenumbers [47], electron donating co-adsorbates (like H) lower these frequencies. Looking at the frequency of linearly and bridge-bonded CO at 2084 and 1841 cm⁻¹ and comparing with the results we received from the CO-TPIR experiments at 50 °C (2080 cm⁻¹ for linearly and 1836 cm⁻¹ for bridge-bonded CO), we identify a shift

of 4 and 5 cm⁻¹ to higher wavenumbers. Thus we can further say that water dissociates on Pt to form OH-groups. After adding CO to the gas feed these OH-groups remain on the surface and induce this blueshift. For the signal at 2168 cm⁻¹ we need a different explanation. Kondo et al. observed a similar feature after low-temperature adsorption of CO on γ-Al₂O₃ and assigned this signal to CO adsorbed on non-acidic OH-groups [48]. Due to the constant supply of H₂O and CO in our experiments we might be able to observe this species even at elevated temperatures. Malpartida et al. on the other hand observed a similar peak for CO adsorption on OH-precovered Pt/γ-Al₂O₃ and assigned this band to CO interacting strongly via H-bonds with surface hydroxy groups [49]. In agreement with their work we assign this vibration to CO molecules adsorbed on Pt interacting with OH-groups or on non-acidic OH-groups on Al₂O₃.

During heating, the intensity of the peak at 1643 cm⁻¹ decreases quickly, showing desorption of physisorbed H₂O. Simultaneously, the intensities of the linear and bridge-bonded CO signals increase and their positions shift to lower frequencies, which is typical for increasing CO coverages on Pt due to the desorption of H₂O or consumption of OH. The CO signal at 2168 cm⁻¹ is not stable and decreases in intensity until it vanishes completely at temperatures above 200 °C. The fact that the position of this signal is not shifting with increasing temperature reinforces the assumption of short range interactions with OH groups on Pt particles or the oxide which are independent of coverage.

Additionally, at temperatures around 200 °C, three peaks develop at 1594, 1391, and 1376 cm⁻¹, which we can assign in

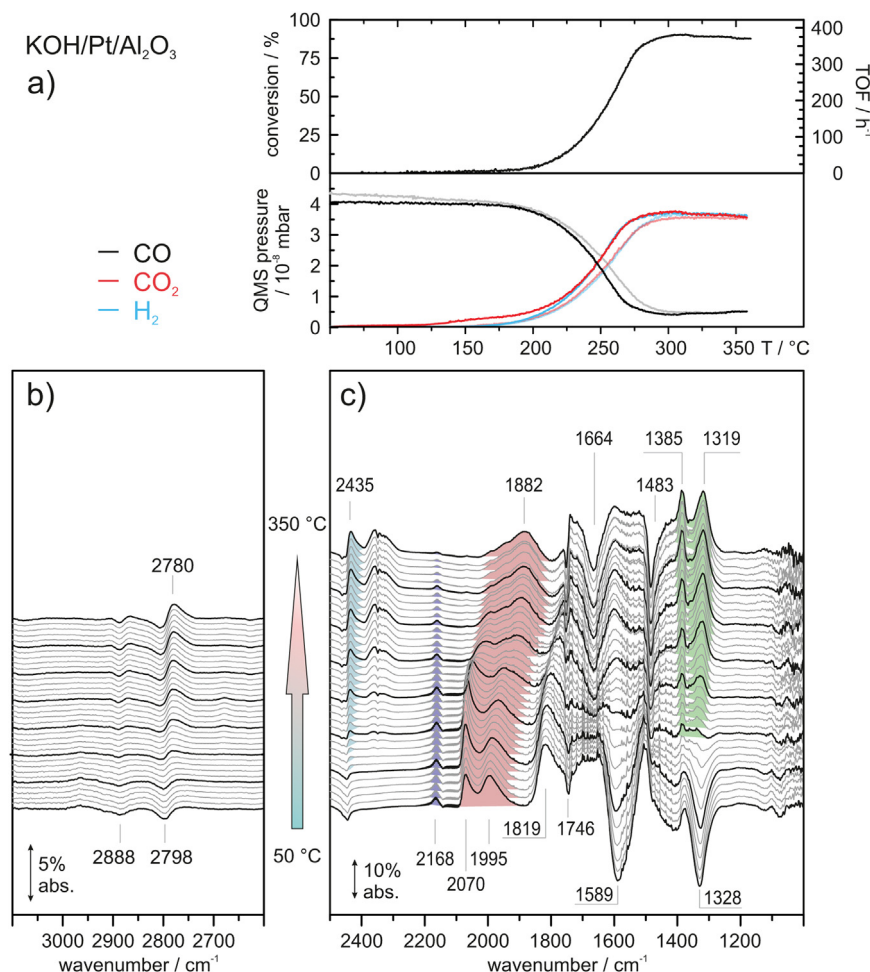


Fig. 5. Online QMS (a) of KOH-coated Pt/Al₂O₃ during temperature-programmed (10 K min⁻¹) WGS reaction and corresponding DRIFT spectra (b and c). Bold lines indicate spectra separated by 50 °C. The reference spectrum was recorded prior to H₂O and CO dosage at 50 °C.

analogy to the results for WGS on Pt-free Al₂O₃ to the $\nu_{as}(\text{OCO})$, $\nu_s(\text{OCO})$, and $\delta_{inplane}(\text{OCH})$ vibrations of the formate ion. This result is in good agreement with previously performed studies on this system where it was shown that formates play a crucial role in the WGSR on Pt [50,51].

3.2.4. KOH/Pt/Al₂O₃

Fig. 5a) shows the QMS data for KOH-coated Pt/Al₂O₃ catalysts during WGS. Remarkably, this catalyst is very active and we observe complete conversion of CO to CO₂ and H₂ with TOFs around 360 h⁻¹ at temperatures above 280 °C. Compared to the uncoated catalyst, H₂-production on the coated catalyst already starts at temperatures around 160 °C, which is about 40 °C lower than on the uncoated sample. In contrast to the uncoated catalyst, CO₂ and H₂ production do not start at the same temperature. Here, CO₂ is released already at lower temperatures before the onset of H₂ production follows. This deviation can only be seen for the heating (opaque lines) and not for the cooling (semi-transparent lines) half-cycle suggesting that the effect is due to the decomposition of species present on the catalyst surface which were not removed in the previous heating cycle.

The spectra of Pt/KOH/Al₂O₃ in the C–H stretching region (Fig. 5b) show only small signals during the whole reaction. In the beginning at 50 °C, two minor negative bands can be seen at 2888 and 2798 cm⁻¹. We assign these features to overtone vibrations of KHCO₂ (potassium formate) which is likely to be formed during the high temperature (350 °C) Ar treatment prior to the

experiment, but quickly decomposes after contact with H₂O [41]. With increasing temperature, we observe the development of a single weak band at 2780 cm⁻¹. For other samples we assigned bands in this region to formates, but the latter typically show two well separated bands. Alternatively the peaks may be due to overtone vibrations of the carbonate anion [52].

In the CO region (Fig. 5c), CO adsorbed on Pt can be seen immediately after dosing. Again, we assign the bands at 2168, 2070, 1995, and 1819 cm⁻¹ to CO adsorbed H-bridge-bonded on Pt with hydroxyl groups (purple) and on oxide species, atop on metallic Pt atoms, atop on Pt atoms influenced by K, and bridge bonded CO on Pt (red), respectively. Further negative bands at 2440, 1746, 1589, and 1328 cm⁻¹ appear after treatment with H₂O at 50 °C. As discussed for WGS on KOH/Al₂O₃, these features (green) arise from the decomposition of mono- and bidentate carbonates and bicarbonates formed during the pretreatment. Up to 175 °C a slight increase and shift to lower wavenumbers of all CO/Pt bands can be seen similar to the one for WGS on Pt/Al₂O₃. Since the intensity grows, this shift cannot be explained by a decreasing CO coverage. Instead, we propose that an increasing hydrogen coverage on the particles may be invoked which leads to the redshift of the CO band. Indeed, Zhou and White showed in temperature-programmed desorption (TPD) experiments a stabilizing effect for hydrogen adsorption on K modified Pt samples [53]. While the desorption activation energy for H on Pt(111) increases significantly at higher K coverage, the saturation coverage of hydrogen decreases. We propose that this behavior has an influence on the WGS reaction. At temperatures

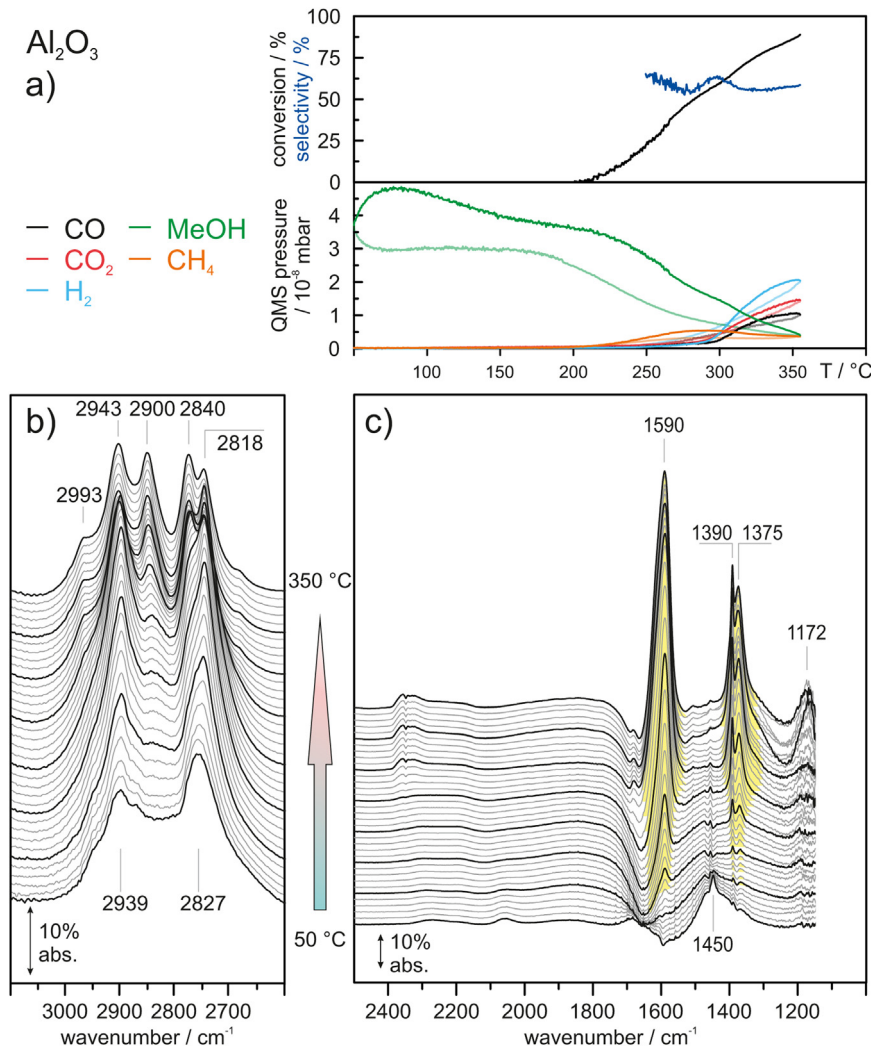


Fig. 6. Online QMS (a) of Al₂O₃ during temperature-programmed (10 K min⁻¹) MSR reaction and corresponding DRIFT spectra (b and c). Bold lines indicate spectra separated by 50 °C. The reference spectrum was recorded prior to MeOH and H₂O dosage at 50 °C.

exceeding 175 °C, the shifts of the CO bands become more pronounced and the intensities start to decrease, which is characteristic for a decreasing CO coverage. [26,54,55] At the same time conversion of CO to CO₂ starts as indicated by the CO₂ gas phase signal at 2340 cm⁻¹ and by the QMS data. Only the CO signal at 2168 cm⁻¹ does not undergo a temperature dependent shift. This indicates that the influence of K on these sites is small, which is in line with the assignment of weakly bound CO to OH on oxide sites or adjacent to OH groups on Pt. At temperatures above 280 °C complete conversion of CO is achieved. At even higher temperatures no further changes in the CO region can be detected. Also the signals of the CO atop bands cannot be separated anymore. For the WGS reaction on Pt/Al₂O₃ we observed the formation of formates whereas for the coated catalyst these bands are absent. Instead, positive signals at 2450, 1746, 1590, 1385, and 1319 cm⁻¹ appear with increasing reaction temperature. We already assigned the bands at 2450 and 1746 cm⁻¹ (blue) to vibrations of K₂CO₃. The other bands at lower wavenumbers can be attributed to mono- or bidentate carbonates and bicarbonates which are formed at elevated temperatures.

In summary, the WGS reaction on KOH-treated Pt/Al₂O₃ shows much lower onset temperature and reaches equilibrium above 280 °C. No formates are observed but instead different carbonate and bicarbonate species are formed with increasing temperature. The coverage and adsorption sites of CO on Pt for the coated catalyst

show a significant temperature dependence. After the onset temperature of the WGS reaction, the coverage of CO on Pt is strongly decreased while CO on K-influenced Pt mostly remains.

3.3. Methanol steam reforming

The MSR activity was measured for all four samples in a similar setup. As for the WGS reaction, the experiments were performed on samples with and without Pt particles both KOH-coated and uncoated in a temperature-programmed experiment with a constant feed of 3.3% MeOH and 6.7% H₂O in Ar.

3.3.1. Al₂O₃

Fig. 6a) shows the QMS data obtained for the reaction in the temperature range of 50–350 °C for the reference sample Al₂O₃. In contrast to the WGS reaction described in the previous section, Al₂O₃ is indeed active for H₂ production at temperatures above 250 °C under the conditions applied. The low amount of CO₂ production leads to a low selectivity (60%) and originates rather from methanol decomposition on Al₂O₃ than steam reforming. The small increase in the MeOH signal in the beginning of the ramp is assigned to MeOH desorbing undecomposed from the material and the overall hysteresis of the MeOH curve can be explained by adsorption and

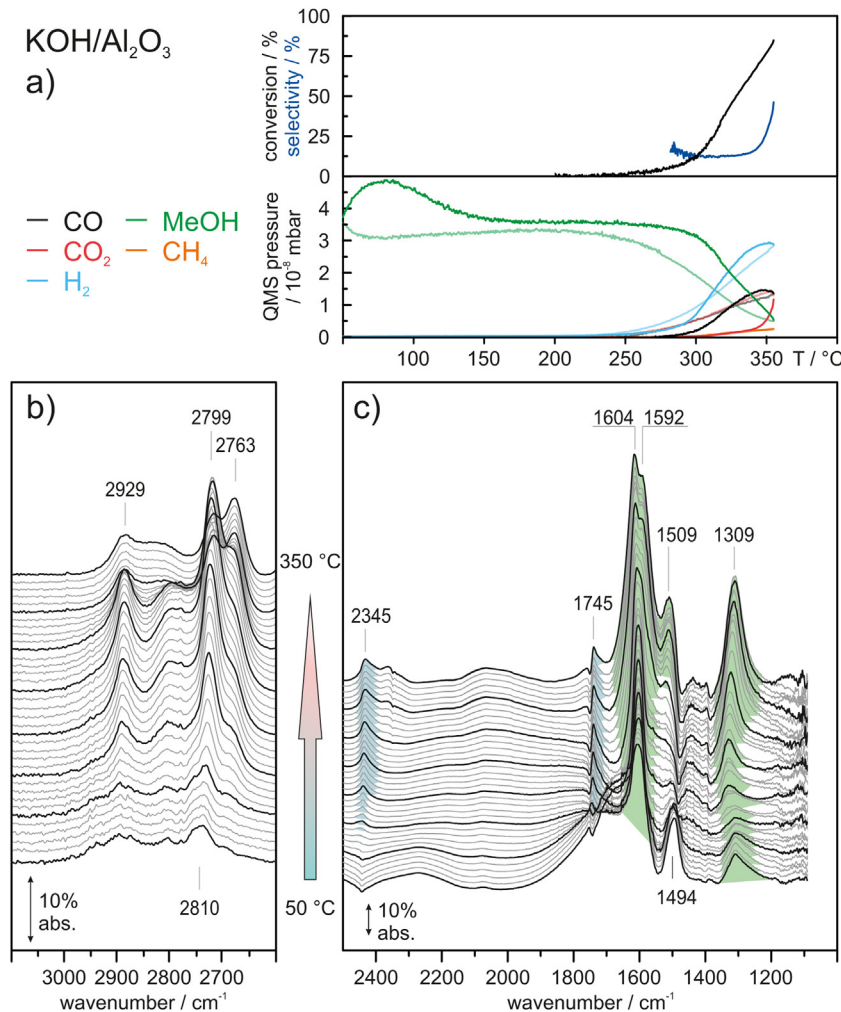


Fig. 7. Online QMS (a) of KOH-coated Al_2O_3 during temperature-programmed (10 K min^{-1}) MSR reaction and corresponding DRIFT spectra (b and c). Bold lines indicate spectra separated by 50°C . The reference spectrum was recorded prior to MeOH and H_2O dosage at 50°C .

desorption processes from the gas supply system, which blur and time-delay the data.

The IR data in Fig. 6b) shows two broad signals centered at 2939 and 2827 cm^{-1} in the C–H stretching area after co-adsorption of MeOH and H_2O , most likely due to several overlapping bands of mono- and multilayer signals. The intensities of these signals grow with increasing temperature and the peaks separate into 5 clearly distinguishable features. The three signals at 2943 , 2840 , and 2818 cm^{-1} can be assigned to a Fermi resonance of the symmetric C–H vibration and to bending overtones of methoxy groups bound to Al_2O_3 [56]. The other two signals, which appear during heating at 2993 and 2900 cm^{-1} can be assigned to C–H vibrations of surface formates [11,57]. In the wavenumber range between 2500 and 1000 cm^{-1} , only small diffuse signals can be seen at low temperatures. A small and broad positive peak at 1640 cm^{-1} which disappears quickly and becomes even negative at temperatures above 100°C can be assigned to adsorbed water. The negative shape suggests that not all water was removed during the pretreatment of the catalyst and therefore water was already present while the background spectrum was recorded. The other feature present at low temperatures centered around 1450 cm^{-1} disappears quickly upon heating. It corresponds to C–H bending modes of methoxy groups and physisorbed MeOH. After desorption of MeOH only a small amount of methoxy remains on the surface. During heating, three bands appear simultaneously at 1590 , 1390 , and 1375 cm^{-1} . In good agreement with the literature and our results of WGS on

Al_2O_3 , these bands can be assigned to formates ($\nu_{\text{as}}(\text{OCO})$, $\nu_{\text{s}}(\text{OCO})$, and $\delta_{\text{inplane}}(\text{OCH})$, resp.) adsorbed on the oxide [40]. Additionally, these bands develop and grow in intensity at the same temperature as the corresponding formate bands in the CH-region. Once a temperature of 250°C is reached, where MeOH is converted to H_2 , CO, and CO_2 according to the QMS data, the intensity of these bands stops growing and instead decreases again.

In summary, MSR on Al_2O_3 without a noble metal catalyst shows only poor activity and selectivity, which can be mostly attributed to the MeOH decomposition reaction on the pristine support. At low temperatures the major part of the surface is occupied by MeOH or methoxy and water while these components desorb quickly during heating. At elevated temperatures ($>100^\circ\text{C}$) MeOH decomposes on Al_2O_3 to formates, which are stable up to 250°C . Subsequently, the decomposition of these formates starts while their concentration on the surface decreases slightly.

3.3.2. KOH/ Al_2O_3

The KOH-coated Al_2O_3 shows similar performance as the uncoated material in the QMS data. At temperatures below 250°C , no conversion of MeOH is seen in the spectra (Fig. 7a). Interestingly, the rate of CO_2 -production shows a significant hysteresis for both cycles. While almost no CO_2 is released during the heating half-cycle, during the cooling half-cycle the curve for CO_2 is in line with the data for CO and H_2 . This behavior may indicate that a part of the CO_2 produced during heating is converted to a surface bound

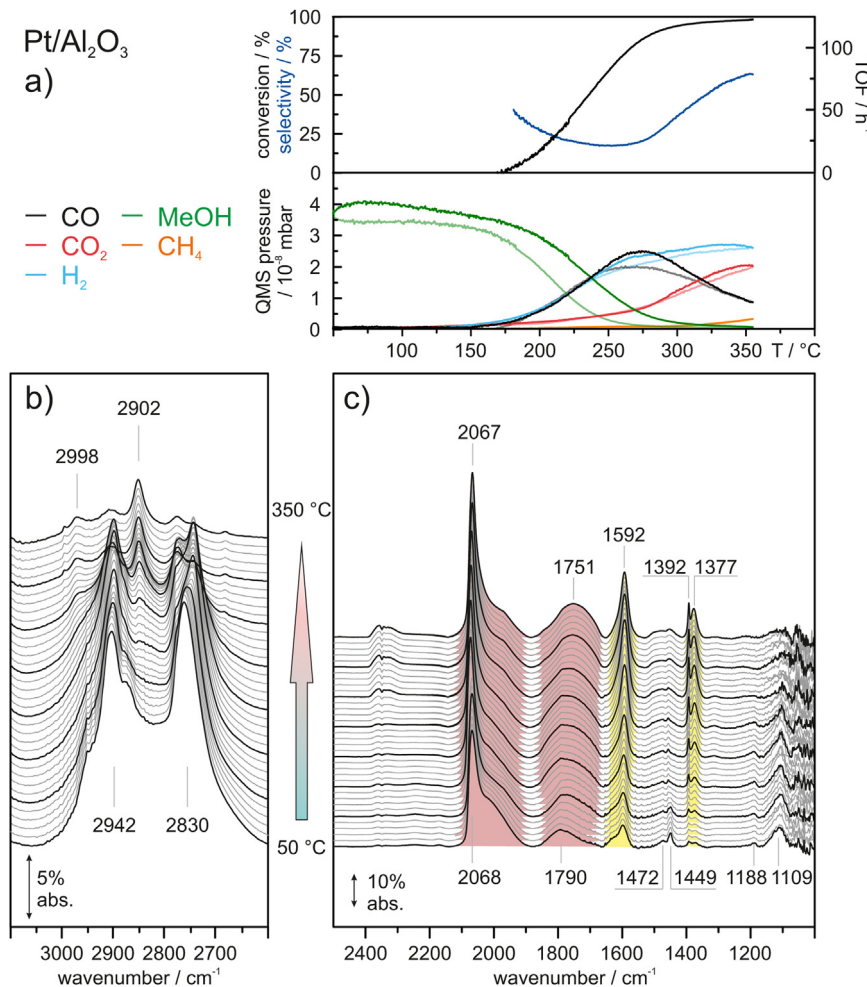


Fig. 8. Online QMS (a) of Pt/Al₂O₃ during temperature-programmed (10 K min⁻¹) MSR reaction and corresponding DRIFT spectra (b and c). Bold lines indicate spectra separated by 50 °C. The reference spectrum was recorded prior to MeOH and H₂O dosage at 50 °C.

species on the KOH-treated support. Also, the very low selectivity (below 50%) suggests that mainly methanol decomposition takes place on this catalyst.

The IR spectra in the C–H stretching region (Fig. 6b) show only small and very broad signals at low temperatures. During heating, the distinct features are clearly visible in this region and we assign them to vibrations of methoxy or MeOH adsorbed on Al₂O₃. The vast shift of the bands compared to pristine Al₂O₃ can be explained by the presence of K-ions on the surface. Even et al. already demonstrated that alkali atoms (e.g. salt coatings containing alkali atoms) have an immense effect on the vibrational frequencies of C–H bonds shifting them to lower wavenumbers [11]. They also suggested that the weakening of C–H bonds by alkali doping can drastically improve the performance of catalysts for WGS or MSR reaction. Interestingly, no features representing formates can be seen in this region. In the range from 2500 to 1000 cm⁻¹ (Fig. 7b), peaks at 2435, 1745, 1604, 1592, 1509, and 1309 cm⁻¹ develop in the spectra with increasing temperature. The same signals were already observed under WGS conditions on the same catalyst and can be attributed to vibrations of K₂CO₃ species (blue) and carbonates (green) on the surface. This observation is in fairly good agreement with the QMS data, where we observe a strong hysteresis for CO₂ production during the heating cycle. The signals referring to carbonates lose intensity during the last 50 °C of the heating ramp, and simultaneously CO₂ evolution starts from the decomposition of the carbonates. Therefore, we assume that on the

coated support under MSR conditions, carbonates are formed from CO₂ initially which decompose to CO₂ at higher temperatures.

3.3.3. Pt/Al₂O₃

The results for the activity of the Pt/Al₂O₃ catalyst is shown in Fig. 8a). Compared with the metal-free catalyst, H₂ evolution starts on Pt particles at quite low temperatures of 175 °C. Simultaneously, MeOH is converted and the main carbon containing product in the initial stage between 150 and 250 °C is CO while only a small increase of CO₂ production can be seen with selectivities below 25%. At temperatures above 270 °C, where MeOH is completely converted and a maximum TOF of 120 h⁻¹ is reached, the rate for CO production decreases again. Remarkably, from this point on, the rates for CO₂ and H₂ production keep increasing further and thus improving the selectivity up to 62% at 350 °C. This behavior can be explained by considering the onset of the WGS reaction on Pt above 270 °C, where CO reacts with H₂O to form CO₂ and a further equivalent of H₂. This is also in good agreement with the previous experiment, where the WGS reaction on Pt/Al₂O₃ showed initial activity in the same temperature range.

The spectra in the C–H stretching region (Fig. 8b) show a very similar structure as for the metal-free oxide under MSR conditions. At low temperatures, only the bands for physisorbed MeOH or bound methoxy (2942 and 2830 cm⁻¹) can be observed, while at elevated temperatures these bands lose intensity and formate bands (2998 and 2902 cm⁻¹) become visible. The region between 2500 and 1000 cm⁻¹ shows also very similar features to the spectra

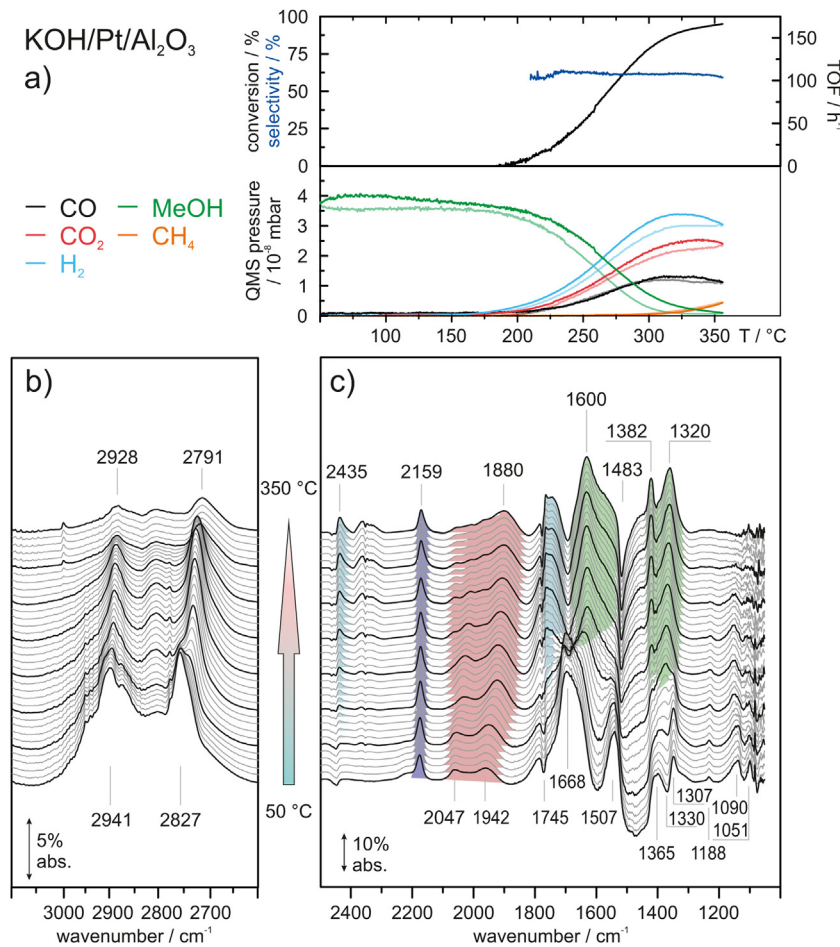


Fig. 9. Online QMS (a) of Pt/Al₂O₃ during temperature-programmed (10 K min⁻¹) MSR reaction and corresponding DRIFT spectra (b and c). Bold lines indicate spectra separated by 50 °C. The reference spectrum was recorded prior to MeOH and H₂O dosage at 50 °C.

we received of the WGS reaction on Pt/Al₂O₃. At low temperatures bands for CO adsorbed on Pt (red) in linear (2068 cm⁻¹) and bridging coordination (1790 cm⁻¹) from the MeOH decomposition reaction can be seen. The total intensities of these peaks are rather small compared to the corresponding peaks for the WGS reaction. Furthermore, the intensity of the atop peak increases with increasing reaction temperature while the position stays constant over the whole temperature range. As discussed previously, the position of the peak is dependent of the CO coverage and presence of co-adsorbates on the particles. The fact that the peak intensity increases with temperatures suggests an increase of CO coverage at higher temperatures due to desorption of co-adsorbed species. Usually, an increasing CO coverage on metals is accompanied by a blueshift of the vibrational frequency. Since the peak position stays constant we may assume that an electron density withdrawing co-adsorbate (like OH⁻ or O⁻) desorbs to free adsorption sites. Further signals in this region can be seen at 1592, 1472, 1449, 1392, 1377, and 1109 cm⁻¹. As for the WGS reaction and for MSR on Pt/Al₂O₃, the features at 1592, 1392, and 1377 cm⁻¹ (yellow) can be assigned to surface formates. The weak signals at 1472 and 1449 cm⁻¹ can be assigned to C—H deformation vibrations ($\delta_{as}(\text{CH}_3)$ and $\delta_s(\text{CH}_3)$) and the feature at 1109 cm⁻¹ to C—O stretching vibrations ($\nu(\text{CO})$) of methoxy groups which desorb at low temperature [58,59]. The onset of the WGS reaction, which is responsible for the higher selectivity, can also be seen in the decrease of the formate band intensity in the spectra above 280 °C.

3.3.4. KOH/Pt/Al₂O₃

Finally, the reactivity and selectivity data on the KOH-coated catalyst is depicted in Fig. 9a). Surprisingly, the coated catalyst has a higher onset temperature than the uncoated one and the conversion of MeOH starts at similar temperatures (200 °C) as the WGS reaction on this catalyst. During the initial phase between 200 and 300 °C the production rates for CO and CO₂ are quite similar as can be seen from the throughout high selectivity of 64%. At temperatures above 300 °C the amount of CO decreases again. This can be caused due to two different side reaction at elevated temperatures. Methane can be produced via the Sabatier reaction which converts CO₂ and H₂ to CH₄ and H₂O. In the first place this leads to a decrease of CO₂ concentration in the product gas stream but because of the improved WGS activity CO can react further with the produced H₂O to recover CO₂ and H₂. The other side reaction is the energetically favored methanation reaction, where CO and H₂ form CH₄ and H₂O.

The IR data of the C—H stretching region (Fig. 9b) show some interesting differences in comparison to the uncoated catalyst. At 50 °C, both spectra for the coated and uncoated Pt catalyst exhibit peak structures with strong similarities regarding intensity ratios and peak positions, indicating multilayer adsorption of MeOH on the catalyst. As the temperature is increased, a strong temperature-dependent shift of the band at 2827–2791 cm⁻¹ is observed. The redshift of the C—H vibrational frequency can be explained by the influence of K and was discussed above for MSR on Al₂O₃/KOH. Remarkably, the most prominent difference between the uncoated

and coated catalyst in MSR is the absence of formate C–H stretching bands in the spectra of the coated catalyst.

The observed features in the range of 2500–1000 cm⁻¹ look similar to the spectra we obtained for the WGS reaction on this catalyst. At 50 °C MeOH already decomposes to CO and we observe bands for linearly adsorbed CO on Pt at 2047 cm⁻¹ and K-influenced Pt at 1942 cm⁻¹. Comparison with the same catalyst under the condition of the WGS reaction shows a significant redshift of these bands by 23 and 53 cm⁻¹, respectively. Likewise, the signal for CO bound in bridge configuration undergoes a very strong redshift so that it cannot be separated anymore from the strong absorption signal of H₂O at 1668 cm⁻¹. Since H₂O is a common reagent for both, the WGS and MSR reaction, the decomposition of MeOH is mainly responsible for this shift. We assume that during decomposition, hydrogen is formed on the particles. Indeed, when hydrogen and CO are co-adsorbed on Pt, a redshift of the CO-signal is expected. This assumption is confirmed by the fact that the CO signal intensity is significantly lower compared to the WGS reaction. The development of the signal structure with temperature is similar to the WGS reaction. Actually, at the maximum temperature, the peak shape, intensity, and position (1882 cm⁻¹ for WGS vs 1880 cm⁻¹ for MSR) of the CO signal are in very good agreement, since hydrogen is produced as well in the WGS reaction at elevated temperatures and contributes to the redshift of adsorbed CO. The signal for CO interacting with OH-groups via H-bonding at 2159 cm⁻¹ is clearly visible during the whole course of the experiment in contrast to the uncoated catalyst [48,49]. This emphasizes the importance of the availability of OH groups on the metal during steam reforming to achieve high selectivities and conversion.

The complex signal structure in the range 1800–1300 cm⁻¹ was previously discussed and is attributed to the formation of mono- and bidentate carbonates and bicarbonates. Weak bands below 1200 cm⁻¹ show the initial formation of methoxy groups which quickly decompose after the onset of the reaction. At higher wavenumbers, the characteristic bands for K₂CO₃ can be observed in analogy to the other experiments of the coated catalyst at 2435 and 1745 cm⁻¹.

4. Conclusions

We have employed combined temperature-programmed DRIFTS and online-QMS to study the catalytic behavior of KOH-coated Pt catalysts for the WGS and MSR reaction under operando conditions.

The addition of K has a drastic effect on the electronic structure of Pt particles. CO adsorbed on K-modified Pt undergoes a strong shift to lower wavenumbers. This holds for CO on both on atop and on bridge positions. The shift can be understood as weakening of the C–O bond while simultaneously strengthening the Pt–C bond. This leads to hindrance for desorption of CO from Pt while facilitating the reaction of CO with OH to form CO₂. Additionally, CO is depleted from atop sites while the amount of CO on bridge sites is increases. At temperatures of 350 °C adsorbed CO can be completely removed from the uncoated catalyst while a small amount of CO is still stable on the coated one.

For the WGS reaction, the onset temperature for reaction is lowered by approximately 40 °C, indicating an increase in activity by addition of KOH. The IR data provides evidence for a change in the reaction mechanism from a formate driven one on the uncoated system to a more selective one on the KOH-coated catalyst involving mainly carbonates as the most abundant surface species. The increased activity is associated to the availability of OH groups on the metal which is increased on the coated catalyst.

The MSR reaction is unselective (<25%) on the uncoated catalyst up to temperatures that allow conversion of CO to CO₂ via the WGS

reaction. The coated catalyst shows high selectivity (64%) over the whole temperature range. Here, unselective MeOH decomposition to CO is prevented, because the onset of the WGS reaction is lower than the onset temperature for MSR.

In conclusion our experiments demonstrate that the very simple and cheap coating of Al₂O₃ supported Pt catalysts with KOH has a strong influence on both the WGS and MSR reactions. This modification can be understood in terms of K-doping of the Pt component thereby modifying the electronic structure of the noble metal. This affects the reaction pathway, the dominant surface intermediates, the onset temperatures and, thereby, also the selectivity of the reaction.

Acknowledgements

AK, ML and JL acknowledge financial support by the Deutsche Forschungsgemeinschaft (DFG) within the Excellence Cluster “Engineering of Advanced Materials” in the framework of the excellence initiative and additional support by the COST Action CM1104. MK and PW thank for financial support of the European Research Council (ERC) under the Advanced Investigator Grant No. 267376.

References

- [1] U. Eberle, M. Felderhoff, F. Schüth, Angew. Chem. 121 (2009) 6732–6757.
- [2] G.A. Olah, A. Goepert, G.K.S. Prakash, *Beyond Oil and Gas: The Methanol Economy*, Wiley-VCH Verlag GmbH & Co KGaA, Weinheim, Germany, 2009.
- [3] B. McNicol, J. Power Sources 100 (2001) 47–59.
- [4] B. Lindström, Int. J. Hydrogen Energy 26 (2001) 923–933.
- [5] J. Shen, Catal. Today 77 (2002) 89–98.
- [6] A. Iulianelli, P. Ribeirinha, A. Mendes, A. Basile, Renew. Sustain. Energy Rev. 29 (2014) 355–368.
- [7] S. Sá, H. Silva, L. Brandão, J.M. Sousa, A. Mendes, Appl. Catal. B 99 (2010) 43–57.
- [8] B. Liu, T. Huang, Z. Zhang, Z. Wang, Y. Zhang, J. Li, Catal. Sci. Technol. 4 (2014) 1286.
- [9] Y. Zhai, D. Pierre, R. Si, W. Deng, P. Ferrin, A.U. Nilekar, G. Peng, J.A. Herron, D.C. Bell, H. Saltsburg, M. Mavrikakis, M. Flytzani-Stephanopoulos, Science 329 (2010) 1633–1636.
- [10] J.M. Pigos, C.J. Brooks, G. Jacobs, B.H. Davis, Appl. Catal. A 328 (2007) 14–26.
- [11] H.N. Evin, G. Jacobs, J. Ruiz-Martinez, U.M. Graham, A. Dozier, G. Thomas, B.H. Davis, Catal. Lett. 122 (2008) 9–19.
- [12] J.C. Bertolini, P. Delichère, J. Massardier, Surf. Sci. 160 (1985) 531–541.
- [13] J.E. Crowell, E.L. Garfunkel, G.A. Somorjai, Surf. Sci. 121 (1982) 303–320.
- [14] E.L. Garfunkel, J.E. Crowell, G.A. Somorjai, J. Phys. Chem. 86 (1982) 310–313.
- [15] J.H. Pazmiño, M. Shekhar, W. Damion Williams, M. Cem Akatay, J.T. Miller, W. Nicholas Delgass, F.H. Ribeiro, J. Catal. 286 (2012) 279–286.
- [16] M. Kusche, F. Enzenberger, S. Bajus, H. Niedermeyer, A. Bösmann, A. Kaftan, M. Laurin, J. Libuda, P. Wasserscheid, Angew. Chem. Int. Ed. 52 (2013) 5028–5032.
- [17] M. Kusche, F. Agel, N. Ní Bhriain, A. Kaftan, M. Laurin, J. Libuda, P. Wasserscheid, ChemSusChem 7 (2014) 2516–2526.
- [18] M. Kusche, K. Bustillo, F. Agel, P. Wasserscheid, ChemCatChem 7 (2015) 766–775.
- [19] H. Li, M. Rivallan, F. Thibault-Starzyk, A. Travert, F.C. Meunier, Phys. Chem. Chem. Phys. 15 (2013) 7321–7327.
- [20] D.R. Lide, CRC Handbook of Chemistry and Physics: A Ready-Reference Book of Chemical and Physical Data, 89th ed., CRC, Boca Raton, Fla., London, 2008.
- [21] F. Meunier, D. Reid, A. Goguet, S. Shekhtman, C. Hardacre, R. Burch, W. Deng, M. Flytzanistphanopoulos, J. Catal. 247 (2007) 277–287.
- [22] J.M. Olinger, P.R. Griffiths, Anal. Chem. 60 (1988) 2427–2435.
- [23] B.E. Heyden, A.M. Bradshaw, Surf. Sci. 125 (1983) 787–802.
- [24] N.R. Avery, Appl. Surf. Sci. 13 (1982) 171–179.
- [25] C.W. Olsen, R.I. Masel, Surf. Sci. 201 (1988) 444–460.
- [26] P. Hollins, Surf. Sci. Rep. 16 (1992) 51–94.
- [27] F. Hoffmann, Surf. Sci. Rep. 3 (1983) 107.
- [28] H.A. Al-Abadleh, V.H. Grassian, Langmuir 19 (2003) 341–347.
- [29] A.M. Turek, I.E. Wachs, E. DeCanio, J. Phys. Chem. 96 (1992) 5000–5007.
- [30] N.D. Parkyns, J. Phys. Chem. 75 (1971) 526–531.
- [31] H.P. Bonzel, Surf. Sci. Rep. 8 (1988) 43–125.
- [32] Z.M. Liu, Y. Zhou, F. Solymosi, J.M. White, Surf. Sci. 245 (1991) 289–304.
- [33] Y. Kinomoto, S. Watabane, M. Takahashi, M. Ito, Surf. Sci. 242 (1991) 538–543.
- [34] B. Krupay, J. Catal. 67 (1981) 362–370.
- [35] M.J. Genge, A.P. Jones, G. Price, Geochim. Cosmochim. Acta 59 (1995) 927–937.
- [36] K. Buijs, C. Schutte, Spectrochim. Acta 17 (1961) 917–920.
- [37] C.M. Greenlieff, P.L. Radloff, S. Akhter, J.M. White, Surf. Sci. 186 (1987) 563–582.
- [38] Y. Amenomiya, J. Catal. 57 (1979) 64–71.
- [39] V. Boidajiev, W.T. Tysoe, Chem. Mater. 10 (1998) 334–344.

- [40] G.G. Olympiou, C.M. Kalamaras, C.D. Zeinalipour-Yazdi, A.M. Efstathiou, *Catal. Today* 127 (2007) 304–318.
- [41] J. Maas, *Spectrochim. Acta Part A* 34 (1978) 179–180.
- [42] E. Spinner, *Spectrochim. Acta Part A* 31 (1975) 1545–1546.
- [43] T.L. Charlton, K.B. Harvey, *Can. J. Chem.* 44 (1966) 2717–2727.
- [44] J.M. Pigos, C.J. Brooks, G. Jacobs, B.H. Davis, *Appl. Catal. A* 319 (2007) 47–57.
- [45] P. Bazin, O. Saur, J.C. Lavalley, M. Daturi, G. Blanchard, *Phys. Chem. Chem. Phys.* 7 (2005) 187.
- [46] H. Bonzel, G. Pirug, J. Müller, *Phys. Rev. Lett.* 58 (1987) 2138–2141.
- [47] Y. Barshad, X. Zhou, E. Gulari, *J. Catal.* 94 (1985) 128–141.
- [48] J.N. Kondo, R. Nishitani, E. Yoda, T. Yokoi, T. Tatsumi, K. Domen, *Phys. Chem. Chem. Phys.* 12 (2010) 11576–11586.
- [49] I. Malpartida, M. Vargas, L. Alemany, E. Finocchio, G. Busca, *Appl. Catal. B* 80 (2008) 214–225.
- [50] G. Jacobs, L. Williams, U. Graham, D. Sparks, B.H. Davis, *J. Phys. Chem. B* 107 (2003) 10398–10404.
- [51] G. Jacobs, *Appl. Catal. A* 252 (2003) 107–118.
- [52] J.A. Goldsmith, S.D. Ross, *Spectrochim. Acta Part A* 23 (1967) 1909–1915.
- [53] X.-L. Zhou, J.M. White, *Surf. Sci.* 185 (1987) 450–456.
- [54] S.C. Chang, L.-W.H. Leung, M.J. Weaver, *J. Phys. Chem.* 93 (1989) 5341–5345.
- [55] R.M. Hammaker, S.A. Francis, R.P. Eischens, *Spectrochim. Acta* 21 (1965) 1295–1309.
- [56] J.D. Head, *Int. J. Quantum Chem.* 77 (2000) 350–357.
- [57] C. Choong, Z. Zhong, L. Huang, A. Borgna, L. Hong, L. Chen, J. Lin, *ACS Catal.* 4 (2014) 2359–2363.
- [58] T.P. Beebe, J.E. Crowell, J.T. Yates, *J. Phys. Chem.* 92 (1988) 1296–1301.
- [59] W.-C. Wu, C.-C. Chuang, J.-L. Lin, *J. Phys. Chem. B* 104 (2000) 8719–8724.